

Longitudinal Flow of Protons from 2-8 AGeV Central Au+Au Collisions

J.L. Klay,¹ N.N. Ajitanand,² J.M. Alexander,² M.G. Anderson,¹ D. Best,³ F.P. Brady,¹ T. Case,³ W. Caskey,¹ D. Cebra,¹ J.L. Chance,¹ P. Chung,² B. Cole,⁴ K. Crowe,³ A.C. Das,⁵ J.E. Draper,¹ M.L. Gilkes,⁶ S. Gushue,⁷ M. Heffner,¹ A.S. Hirsch,⁶ E.L. Hjort,⁶ L. Huo,⁸ M. Justice,⁹ M. Kaplan,¹⁰ D. Keane,⁹ J.C. Kintner,¹¹ D. Krofcheck,¹² R.A. Lacey,² J. Lauret,² C. Law,² M.A. Lisa,⁵ H. Liu,⁹ Y.M. Liu,⁸ R. McGrath,² Z. Milosevich,¹⁰ G. Odyniec,³ D.L. Olson,³ S.Y. Panitkin,⁹ C. Pinkenburg,² N.T. Porile,⁶ G. Rai,³ H.G. Ritter,³ J.L. Romero,¹ R. Scharenberg,⁶ L. Schroeder,³ B. Srivastava,⁶ N.T.B. Stone,³ T.J.M. Symons,³ S. Wang,⁹ R. Wells,⁵ J. Whitfield,¹⁰ T. Wienold,³ R. Witt,⁹ L. Wood,¹ and W.N. Zhang⁸

(E895 Collaboration)

¹University of California, Davis, California 95616

²Department of Chemistry and Physics, SUNY, Stony Brook, New York 11794-3400

³Lawrence Berkeley National Laboratory, Berkeley, California 94720

⁴Columbia University, New York, New York 10027

⁵The Ohio State University, Columbus, Ohio 43210

⁶Purdue University, West Lafayette, Indiana 47907-1396

⁷Brookhaven National Laboratory, Upton, New York 11973

⁸Harbin Institute of Technology, Harbin, 150001 People's Republic of China

⁹Kent State University, Kent, Ohio 44242

¹⁰Carnegie Mellon University, Pittsburgh, Pennsylvania 15213

¹¹St. Mary's College of California, Moraga, California 94575

¹²University of Auckland, Auckland, New Zealand

(Dated: October 23, 2018)

Rapidity distributions of protons from central $^{197}\text{Au} + ^{197}\text{Au}$ collisions measured by the E895 Collaboration in the energy range from 2 to 8 AGeV at the Brookhaven AGS are presented. Longitudinal flow parameters derived using a thermal model including collective longitudinal expansion are extracted from these distributions. The results show an approximately linear increase in the longitudinal flow velocity, $\langle\beta\gamma\rangle_L$, as a function of the logarithm of beam energy.

PACS numbers: PACS numbers: 25.75.-q, 25.60.Gc, 25.75.Ld

Experimental heavy ion programs from the Bevalac, SIS, the AGS and the CERN SPS have attempted to characterize the distributions of particles emerging from high energy collisions in terms of simple thermodynamic principles. Testing the underlying assumptions of chemical and thermal equilibrations at different stages of the collision has been attempted by comparing model expectations to many different experimental observables. Static isotropic thermal emission models applied to observed particle rapidity distributions from experiments at all beam energies consistently fail to describe the observed shape; such model predictions being too narrow. Thermal models which include collective longitudinal expansion have been much more successful at reproducing the observed rapidity distributions [1, 2]. The additional collective motion is attributed to intense pressure gradients which develop in the very hot, compressed nuclear matter fireballs created in heavy ion collisions.

At the AGS, rapidity distributions of multiple particle species, including pions, kaons, protons and lambda hyperons from central collisions have been simultaneously described by a thermal distribution with a common longitudinal expansion velocity [2, 3]. The agreement between the proton and other particle distributions suggests a high degree of stopping of the incident nucleons

at the top AGS energy, which implies even more stopping at lower beam energies. However, recent investigations of the centrality dependence of the proton rapidity distributions from 6-11 AGeV Au+Au collisions by E917 suggest that the degree of nucleon stopping may be less than previously considered [4]. Nevertheless, their flat dN/dy for *central* collisions at all beam energies, fitted by sources distributed uniformly in rapidity to $y-y_{cm} = 0$, could also be interpreted in the manner presented herein.

For the asymptotic case at extremely high beam energies, Bjorken proposed [5] that nuclear transparency would evacuate the central rapidity region of all of the initial nucleons, leaving a hot, high-energy density region in which a Quark Gluon Plasma might form. In 160 AGeV Pb+Pb collisions at the CERN SPS, observed net proton ((+)-(-)) rapidity distributions [6] exhibit a double-humped character which is consistent with this transparency. At SPS energies, the nucleon distributions are not describable by a simple thermal model with only collective longitudinal flow, but rather need additional theoretical consideration of transparency. However, the negative hadron (mostly pions) rapidity distributions are well-described by this model, which might be interpreted as suggesting a significant amount of collective longitudinal flow for produced particles [2].

More recently, models which attempt simultaneously to characterize many of the freeze-out parameters (transverse and longitudinal flow, temperature, chemical potential and source volume) have been attempted on data at and above the top energy at the AGS [7]. The data discussed in this letter are compared only to the locally thermal model with longitudinal flow.

The new data were taken by the E895 Experiment [8] at nominally 2, 4, 6, and 8 AGeV (1.85, 3.91, 6.0 and 8.0 AGeV after correction for energy loss before the target) at the Brookhaven AGS using the EOS TPC [9]. Global characterization of the collisions is made possible by the nearly 4π center of mass frame coverage provided by this detector. Particle identification is achieved by correlating the average ionization energy loss in the P10 drift gas with the charged particle momenta, reconstructed from the curvature of tracks bent by the Multi-Particle Spectrometer (MPS) magnet as they pass through the TPC.

The 5% most central events were selected using the distribution of primary charged particle event multiplicities. Primary tracks are required to originate within 2.5 cm of the reconstructed event vertex. This analysis is based on approximately 20,000 selected central events at each beam energy.

For particle identification [10], all tracks are initially assigned the proton mass and sorted into rapidity and transverse mass bins: 0.1 unit rapidity slices from beam to target rapidity, with the mid-rapidity slice corresponding to $|y - y_{cm}| < 0.05$, and 25 MeV/c² wide transverse mass bins in the range $0 < m_t - m_0 < 1.0$ GeV/c². The mean total momentum and $\beta\gamma$ are computed at the center of the $(m_t - m_0, y)$ bins and are used with a parameterization of the Bethe-Bloch energy loss as a function of $\beta\gamma$ to fit for the relative particle populations in $\langle dE/dx \rangle$ projected for each $(m_t - m_0, y)$ bin. The total yield of protons in each bin is obtained from the area under the fitted proton $\langle dE/dx \rangle$ distribution.

Up to a total momentum, p , of 1 GeV/c, the protons are isolated in $\langle dE/dx \rangle$ and easily identified. Above 1 GeV/c, pions and kaons begin to contaminate the proton sample. Between 6 and 8 GeV/c total momentum, the proton, deuteron and triton $\langle dE/dx \rangle$ distributions significantly overlap each other and their individual yields cannot be resolved. Pion contamination is removed by using the observed ratio of oppositely charged pions in the momentum range up to 1 GeV/c to extrapolate to higher momenta [10]. The relatively cleanly observed negative pion yields, combined with the extrapolated pion ratios, are used to remove the π^+ contamination from the proton distributions above 1 GeV/c. Kaon contamination is eliminated by using the measured kaon results from [11, 12] for the same beam energies. The confusion among protons, deuterons and tritons between 6 and 8 GeV/c results in a broad hole in the final proton spectra, where the proton yields cannot be extracted. Where appropriate, the reported errors for the raw proton yields include

an estimate of the additional uncertainty resulting from the models used to determine the contamination from other particles.

Simulations of the detector response to protons in all regions of phase space were performed using GEANT 3.21. Small samples (≤ 4 tracks per event) of proton tracks with momentum distributions approximating the measured data were embedded into raw events and propagated through the reconstruction chain. A correction for detector efficiency, acceptance and momentum resolution was obtained from the ratio of found GEANT tracks to the simulated input using the same track quality cuts and centrality selection as the data to be corrected. The proton corrections were largest at very backward rapidities, where detector acceptance causes significant losses, and at forward rapidities, where track density is large, and at low transverse mass. However, the corrected spectra, Fig. 1, show very good forward/backward rapidity reflection symmetry.

The transverse mass spectra of the protons in each rapidity slice are shown in Fig. 1. In order to determine yields, these spectra have been fit with the Maxwell-Boltzmann distribution.

$$\frac{1}{2\pi m_t} \frac{d^2 N}{dm_t dy} = A(y) m_t e^{-(m_t - m_0)/T(y)}, \quad (1)$$

where $A(y)m_0$ represents the $m_t - m_0 = 0$ intercept and $T(y)$ is the inverse slope parameter. It agrees fairly well at large $m_t - m_0$, but the agreement deteriorates for very low $m_t - m_0$, where transverse flow modifies Eq. (1). However, the resulting systematic overestimate of the total integrated yields obtained from the fits are smaller than the uncertainties in the measured integrated yields, dN/dy .

The rapidity density from Eq. (1) can be obtained by integrating over m_t with an overall normalization parameter, B , as

$$\frac{dN_{th}}{dy}(y) = BT^3 \left(\frac{m^2}{T^2} + \frac{m}{T} \frac{2}{\cosh y} + \frac{2}{\cosh^2 y} \right) e^{(-\frac{m}{T} \cosh y)}. \quad (2)$$

The width of the distribution, Eq. (2), as a function of rapidity for a given emitted particle is a function of the temperature and particle mass only. Using the mid-rapidity inverse slope parameters (uncertainty of 2 MeV) from Eq. (1) to approximate the temperature (Table I) in Eq. (2), this distribution can be compared to the rapidity densities extracted from the integrated transverse mass spectra. The result, shown as dashed lines in Fig. 2, is clearly too narrow to describe our data.

Schnedermann, et al. [1] modeled this increase in the widths as the result of collective longitudinal flow. This assumes that the observed distributions arise from the superposition of multiple boosted individual isotropic, locally thermalized sources at each rapidity, η . This is the longitudinally boost-invariant approach [5] but taken to

E_{beam} (AGeV)	T_0 (MeV/c ²)	η_{max}	$\langle\beta_L\rangle$	$\langle\beta\gamma\rangle_L$	Ref.
1.06 (Au)	80	0.37	0.19	0.194	
1.15 (Au)	92	0.41	0.20	0.204	[14]
2	187	0.570 ± 0.024	0.28	0.292	
4	211	0.889 ± 0.024	0.42	0.463	
6	216	1.049 ± 0.026	0.48	0.547	
8	229	1.104 ± 0.025	0.50	0.577	
6 (Au)	253	0.990	0.46	0.518	[4]
8 (Au)	267	1.086	0.50	0.577	[4]
10.8 (Au)	279	1.166	0.52	0.609	[4]
11 (Au)	130	1.10	0.50	0.577	[2]
14.6 (Si+Al)	120	1.15	0.52	0.609	[3]
158 (Pb)	160	1.99	0.76	1.169	[2]
200 (S)	220	1.70 ± 0.30	0.69	0.953	[1]

TABLE I: Longitudinal flow parameters extracted from fits of Eq. (3) to the proton rapidity densities at 2, 4, 6, and 8 AGeV, using the mid-rapidity proton inverse slope parameters, T_0 . Note that the parameters extracted at the SPS come from produced particles, primarily pions, with comparison among other species, such as kaons and strange baryons suggesting collectivity.

a finite boost, η_{max} . The distributions are

$$\frac{dN}{dy} = \int_{\eta_{min}}^{\eta_{max}} d\eta \frac{dN_{th}}{dy}(y - \eta) \quad (3)$$

where $\eta_{max} = -\eta_{min}$, from symmetry about the center of mass; dN_{th}/dy is Eq. (2) with T from Table I; and N is the number of protons observed. An average longitudinal source velocity can be obtained by averaging over $|\eta|$ as $\langle\beta_L\rangle = \tanh(\eta_{max}/2)$.

Fits of this form have been applied to a wide array of experimental data at the AGS and the SPS [1, 2, 3, 13]. Although the inverse slope in Table I is not the true temperature, the longitudinal boost, η_{max} , has been observed to depend only weakly on the temperature input to the model, with the exception of nucleons at SPS energies, which are affected by transparency [1]. In the present data, a 50% decrease in the temperature results in a maximum change of only 15% in η_{max} .

Fits of Eq. (3) to the proton rapidity densities at 2, 4, 6, and 8 AGeV are also shown on Fig. 2. The fit parameter, η_{max} , and the corresponding average velocities, $\langle\beta_L\rangle$, are listed in Table I. $\langle\beta\gamma\rangle_L$ is evaluated by computing $\gamma = 1/\sqrt{1 - \langle\beta_L\rangle^2}$.

Fig. 3 shows our results for $\langle\beta\gamma\rangle_L$ as a function of beam energy. Also included are the extracted parameters from the compiled data from [1, 2, 3, 4, 13, 14].

A modification to a previous interpretation of the lowest energy FOPI data point is presented here. The proton longitudinal flow reported for 1.06 AGeV Au+Au in [2, 13, 15] is from an interpretation of the measured data from [16] which assumed isotropic emission from a

Siemens and Rasmussen [17] radially boosted spherical thermal source. Good agreement between their Au+Au rapidity distributions and predictions from a Siemens-Rasmussen style model based on fits to their mid-rapidity kinetic energy spectra was reported [16]. A temperature of 80 MeV and an average (isotropic) flow velocity of $\langle\beta_r\rangle = 0.41$ were reported.

The resulting longitudinal flow velocity of $\langle\beta\rangle = 0.38$ attributed to the 1.06 AGeV Au+Au data by [2] is a factor of two larger than the value one extracts using the present prescription. The value reported in Table I and Fig. 3 is from our re-analysis of these FOPI 1.06 AGeV rapidity densities using their reported temperature of 80 MeV with Eq. (3). The result is $\langle\beta_L\rangle = 0.19$, which is consistent with a value obtained using the same model with Au+Au collision data measured by the EOS collaboration for $E_{beam}=1.15$ AGeV and reported in [14].

Based on the reported $\langle\beta_L\rangle$ for Au+Au at 1 AGeV and 11 AGeV, a linear relation between $\langle\beta_L\rangle$ and the logarithm of beam energy was suggested [2, 13, 15]. Extrapolated to SPS energies, it did not describe the longitudinal flow at the SPS extracted from produced particles such as pions. However, with the inclusion of the present data from E895 and our re-analysis of the 1 AGeV protons, Fig. 3 shows a linear trend, spanning 1 to 160 AGeV, for the heaviest systems, with a slope ~ 2.5 larger than was previously concluded. The SPS Pb+Pb value (obtained from produced particles, not protons) no longer shows a significant excess above the systematic. Further study of rapidity distributions for protons as a function of centrality [4], and produced particles, with system size and beam energy in the range above the AGS would help to clarify the relation between stopping and longitudinal expansion of protons in heavy ion collisions.

This work was supported in part by the US National Science Foundation under Grants No. PHY-98-04672, PHY-9722653, PHY-96-05207, PHY-9601271, and PHY-9225096; by the U.S. Department of Energy under grants DE-FG02-87ER40331.A008, DE-FG02-89ER40531, DE-FG02-88ER40408, DE-FG02-87ER40324, and contracts DE-AC03-76SF00098, DE-AC02-98CH10886; and by the University of Auckland Research Committee, NZ/USA Cooperative Science Programme CSP 95/33; and by the National Natural Science Foundation of P.R. China under grant number 19875012.

-
- [1] E. Schnedermann, J. Sollfrank and U. Heinz, Phys. Rev. C **48**, 2462 (1993).
 - [2] J. Stachel, Nucl. Phys. A **610**, 509c (1996).
 - [3] P. Braun-Munzinger, J. Stachel, J.P. Wessels, N. Xu, Phys. Lett. B **344**, 43 (1995).
 - [4] B.B. Back, *et al.* (E917 Collaboration), Phys. Rev. Lett. **86**, 1970 (2001).
 - [5] J.D. Bjorken, Phys. Rev. D **27**, 140 (1983).

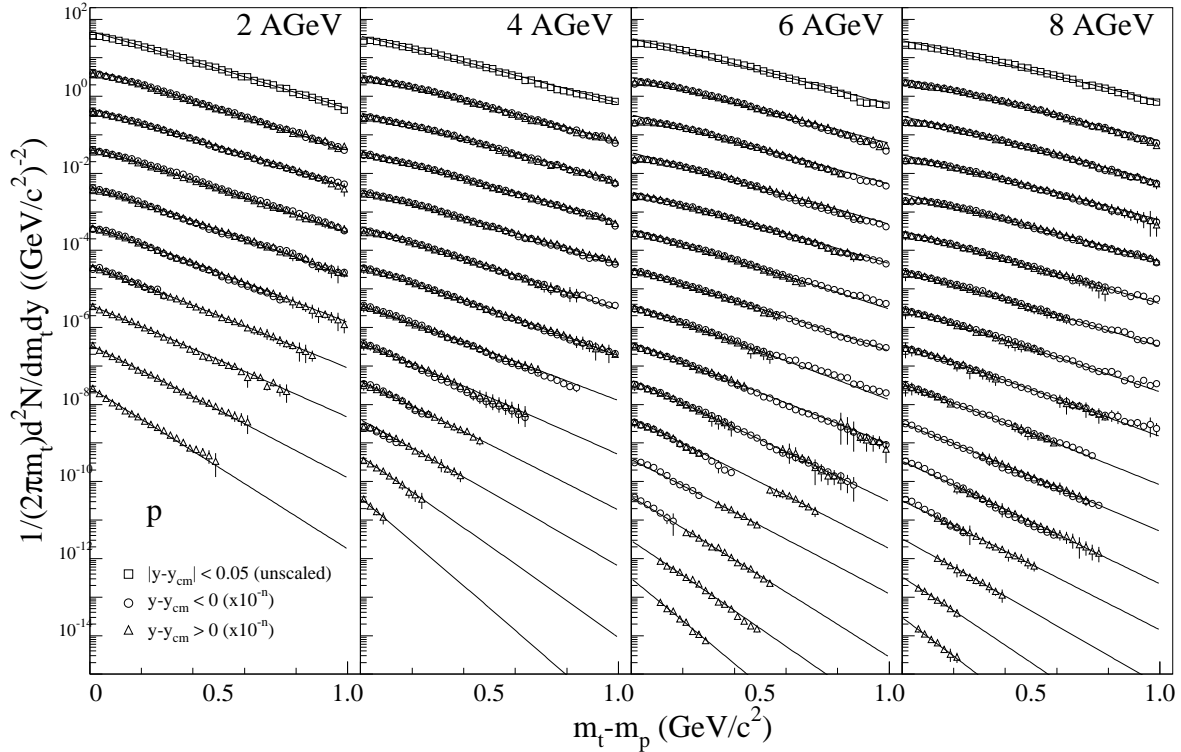


FIG. 1: Invariant yield per event as a function of $m_t - m_p$ for protons in central Au+Au collisions at 2, 4, 6, and 8 AGeV. Midrapidity is shown unscaled, while the 0.1 unit forward/backward rapidity slices are scaled down by successive factors of 10.

- [6] H. Appelshäuser, *et al.*, (NA49 Collaboration), Phys. Rev. Lett. **82**, 2471 (1999).
- [7] Harald Dobler, Josef Sollfrank, Ulrich Heinz, Phys. Lett. B **457**, 353 (1999).
- [8] G. Rai, *et al.*, LBL-PUB-5399 (1993).
- [9] H. Wieman, *et al.*, Nucl. Phys. **A525**, 617c (1991).
- [10] J.L. Klay, Ph.D. Dissertation, University of California, Davis (2001).
- [11] C.A. Ogilvie, Nucl. Phys. A **638**, 57c (1998).
- [12] J.C. Dunlop, Ph.D. Dissertation, Massachusetts Institute of Technology (1999).
- [13] Norbert Herrmann, Johannes P. Wessels, and Thomas Wienold, Annu. Rev. Nucl. Part. Sci. **49**, 581 (1999).
- [14] H. Liu, *et al.*, (E895 Collaboration), Nucl. Phys. A **630**, 549c (1998).
- [15] J.P. Wessels, *Flow Phenomena at AGS Energies*, Talk at the Workshop 'QCD Phase Transitions', Hirschegg, Austria, January 13-18, 1997 (Available at the Los Alamos pre-print server: <http://xxx.lanl.gov/ps/nuclex/9704004>).
- [16] N. Herrmann, (FOPI Collaboration), Nuc. Phys. **A610**, 49c (1996).
- [17] P.J. Siemens and J.O. Rasmussen, Phys. Rev. Lett. **42**, 880 (1979).

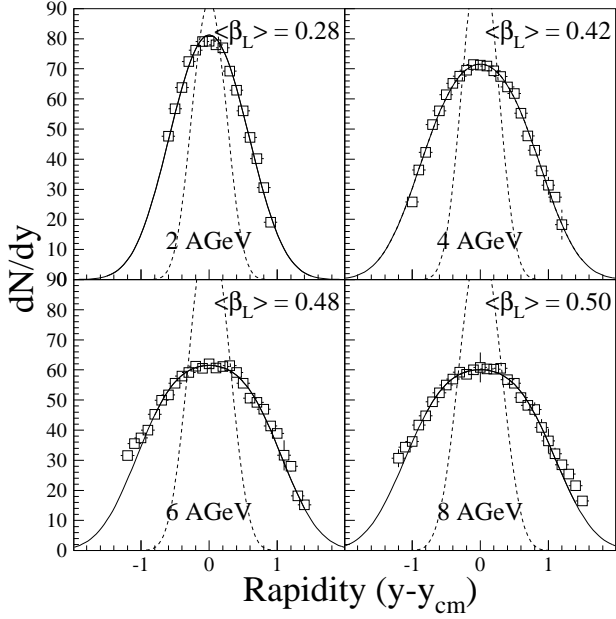


FIG. 2: Proton rapidity distributions in central Au+Au collisions at 2, 4, 6, and 8 AGeV. The dashed curves correspond to isotropic emission from a stationary thermal source with temperatures given by the mid-rapidity inverse slope parameters from the transverse mass fits (Eq. (2)), whereas the solid curves indicate fits with longitudinal flow (Eq. (3)).

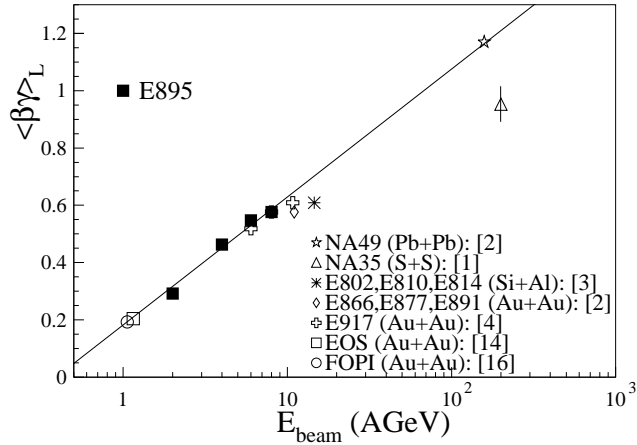


FIG. 3: Energy excitation function of longitudinal flow velocities ($\langle\beta\gamma\rangle_L$), from heavy ion collisions. The open circle has been adjusted here as described in the text. For heavy systems, a roughly linear dependence with respect to $\log_{10}(E_{beam})$ over more than two orders of magnitude of beam energy is illustrated (solid line). Note that the parameters extracted at the SPS come from produced particles, primarily pions, with comparison among other species, such as kaons and strange baryons suggesting collectivity.